

# An Investigation of Capacity Fading of Manganese Spinel Stored at Elevated Temperature

Takao Inoue and Mitsuru Sano

Graduate School of Human Informatics, Nagoya University, Nagoya 464-8601, Japan

## ABSTRACT

The storage characteristics of a manganese spinel at various discharge depths and 80°C were examined in 1 M LiPF<sub>6</sub> ethylene carbonate/dimethyl carbonate (1:2 by volume) electrolyte. The quantities of Mn dissolution and discharge-capacity loss were measured after the cathode at each discharge depth had been exposed to the electrolyte at 80°C. The quantities of dissolved manganese in the solution were less than 1.2% of the total manganese in all cathodes examined. Little capacity fading (3%) was found in the fully charged cathode, but a 59% capacity loss was observed in the fully discharged cathode. Correlations of the capacity loss with the X-ray diffraction peak widths were found, and the amount of capacity loss increased with broadening peak width. On the other hand, no correlation between the amount of Mn dissolution and the capacity loss was found. From these results, we propose a mechanism of the capacity fading of the spinel LiMn<sub>2</sub>O<sub>4</sub> stored at elevated temperatures as follows: lattice defects in the spinel due to Mn dissolution cause disordered crystal structures and as a result, the Li insertion-extraction paths are blocked, leading to capacity fading.

## Introduction

A manganese spinel is one of the most promising cathode (positive electrode) materials used in Li<sub>x</sub>C batteries because of its high theoretical energy density, inexpensive material cost, acceptable environmental characteristics, and good safety.<sup>1-3</sup> Unfortunately, it can exhibit significant capacity fading in cycling or at elevated temperatures.<sup>4-13</sup> Recent improvements in the capacity fading of LiMn<sub>2</sub>O<sub>4</sub> during cycling have been made by Xia and Yoshio,<sup>9</sup> Toso Company (Japan),<sup>14</sup> and Nihon Jukagaku Company (Japan).<sup>15</sup> The manganese spinels now offer the best combination of cost, performance, and safety. Although they exhibit excellent performance at room temperature, much attention is still directed toward efforts to improve their poorer performance at elevated temperatures.<sup>4-13</sup>

Personal electronics in general are not subjected to significant use at elevated temperatures. However, Li-ion batteries in consumer products may be subjected to storage at elevated temperatures, for instance, in unventilated vehicles. Therefore, in order to further the development of the LiMn<sub>2</sub>O<sub>4</sub> spinel as a viable positive-electrode material for Li-ion batteries, it is important to determine the mechanism of the capacity fading during storage at elevated temperatures.

The capacity fading phenomenon is usually linked to the disproportion dissolution of Mn<sup>3+</sup> into the electrolyte. Jang's group<sup>10</sup> quantitatively analyzed the dissolution of Mn into solutions from a spinel during cycling. They reported that the capacity loss occurred via material loss from the spinel and polarization loss due to the cell resistance increase. Xia et al.<sup>12</sup> also studied the capacity fading of a Li/1 M LiPF<sub>6</sub> + ethylene carbonate (EC)/dimethyl carbonate (DMC) (1:2 by volume)/LiMn<sub>2</sub>O<sub>4</sub> cell at elevated temperatures during cycling.

Pistoia et al.<sup>11</sup> reported the storage characteristics of Mn spinels. They studied the influence of such factors as electrolyte, current collector, voltage range, cathode additives, and synthesis conditions on the capacity losses. However, published data on the subject of the storage characteristics of manganese spinels at elevated temperatures is limited.

How much capacity loss does each discharged state in the Mn spinel exhibit at elevated temperatures? What percent of the total capacity loss is due to dissolved Mn? What is the mechanism responsible for capacity fading in manganese spinel stored at high temperatures? These issues require answers before cells with LiMn<sub>2</sub>O<sub>4</sub> electrodes penetrate the battery market.

In this study, in order to gain insight into these problems, the amounts of dissolved Mn and capacity loss were measured for spinel cathodes at selected discharged states stored at 80°C in an electrolyte solution of 1 M LiPF<sub>6</sub> + EC/DMC (1:2 by volume) which is typical for a secondary Li-ion cell.

## Experimental

**Materials.**—Powders of lithium manganese oxides were prepared as described in the following section. Compounds of LiOH·H<sub>2</sub>O (99%) and CH<sub>3</sub>COOH (99%) were purchased from Nakarai Tesque (Kyoto, Japan) and Mn(CH<sub>3</sub>COO)<sub>2</sub>·4H<sub>2</sub>O (99%) from Wako Chemical (Osaka, Japan). A 1:2 mixture of EC and DMC containing 1 M LiPF<sub>6</sub> as the electrolyte salt was purchased from Mitsubishi Chemical (Tokyo, Japan) and contained less than 20 ppm of H<sub>2</sub>O. A conducting binder of acetylene black and poly(tetrafluoroethylene) (PTFE) (2:1) was purchased from Soei Tsusho (Osaka, Japan).

**Instrumentation.**—The amounts of Li and Mn in the as-prepared compound were determined by the usual methods<sup>16</sup> with a Hitachi 180-50 atomic absorption spectrophotometer. The specific surface area was measured by Brunauer-Emmett-Teller (BET) techniques with a Shimadzu Accusorb 2100-01. The crystal structure was determined with a Rigaku RAD X-ray diffractometer with Cu K $\alpha$  radiation monochromated by a graphite crystal. Charge-discharge profiles and performance tests of the cells were recorded with a Nagano BTS-2004 at a galvanostatic current density of 0.5 mA/cm<sup>2</sup>. The cutoff potentials for the charge and discharge were fixed at 4.5 and 3.5 V (vs. Li/Li<sup>+</sup>), respectively.

**Sample preparation.**—Compounds of LiOH·H<sub>2</sub>O (26.2 mmol) and Mn(CH<sub>3</sub>COO)<sub>2</sub>·4H<sub>2</sub>O (50 mmol) were dissolved in a solution of H<sub>2</sub>O (10 mL) and CH<sub>3</sub>COOH (15 mL). The resulting solution was then heated at 80°C for 2 h with stirring and evaporated to dryness at 120°C. The resulting powder was ground in a mortar and calcined at 380°C for 2 h, yielding black solids. This material was then crushed and calcined at 725°C for 24 h. The heating and cooling rates were fixed at 5 and 1°C/min.

**Electrochemical cells.**—Composite cathodes which consisted of 66 wt % spinel powders and 33 wt % conducting binders were pressed carefully at 300 kg/cm<sup>2</sup> and were then dried at 150°C for 2 h. Charge and discharge tests were performed on an assembled cell (Hohsen Co., Osaka, Japan) as Li metal/electrolyte/cathode. All assembling and disassembling of the cells were carried out in an argon-atmosphere glove box (Vacuum Atmospheres Co., CA).

## Results and Discussion

The chemical composition of the prepared Mn spinel compound prepared was Li<sub>1.04</sub>Mn<sub>1.98</sub>O<sub>4</sub> (Li 4.01%, Mn 60.43%) by chemical analysis. X-ray diffraction analyses of the powder showed a spinel structure with no discernable impurities. The crystal structure was indexed to a cubic system with a lattice parameter *a*<sub>0</sub> of 8.234 Å, which was refined with the space group *Fd3m*. The BET specific surface area was 2.67 m<sup>2</sup>/g.

Figure 1 shows an initial charge–discharge curve of a Li/Li<sub>1.04</sub>Mn<sub>1.98</sub>O<sub>4</sub> cell at a current density 0.5 mA/cm<sup>2</sup> between 3.5 and 4.5 V at 25°C. This Mn spinel electrode has an initial charge capacity of 132 mAh/g (the theoretical value is 143 mAh/g). The electrode also shows a discharge capacity of 122 mAh/g with an ordinary two-step voltage profile.

To examine the capacity fading due to elevated temperature, cell performances at 25 and 55°C were tested with a coin cell having a Li<sub>1.04</sub>Mn<sub>1.98</sub>O<sub>4</sub> cathode, a lithium metal anode, and 1 M LiPF<sub>6</sub> in EC:DMC (1:2) electrolyte. The profiles of the charge–discharge curves were similar. Figure 2 shows the decay of the discharge capacity with cycling. After 100 cycles, the discharge capacities at 25 and 55°C were 102 and 84 mAh/g, respectively. Their capacity loss is 15% at 25°C and 28% at 55°C, respectively. The elevated temperature thus accelerates the capacity fading.

**Capacity fading due to manganese loss from Li<sub>1.04</sub>Mn<sub>1.98</sub>O<sub>4</sub> at 80°C.**—The capacity fading at elevated temperatures has been commonly linked to Mn dissolution from the spinel into the electrolyte solution.<sup>4–13,17</sup> There are two likely candidates as causes of the capacity loss: one is manganese loss from the cathode by dissolution and the other is an effect expected due to Mn plating onto the lithium electrode in a solution containing dissolved manganese ions.<sup>18</sup> In order to determine which of the two is the cause of the capacity loss, the cycle performance at room temperature was tested using an electrolyte solution containing manganese ions (23 ppm), where a test cell was constructed with the Li<sub>1.04</sub>Mn<sub>1.98</sub>O<sub>4</sub> cathode as previously described. The performance of this cell was almost equal to that using an ordinary electrolyte solution at

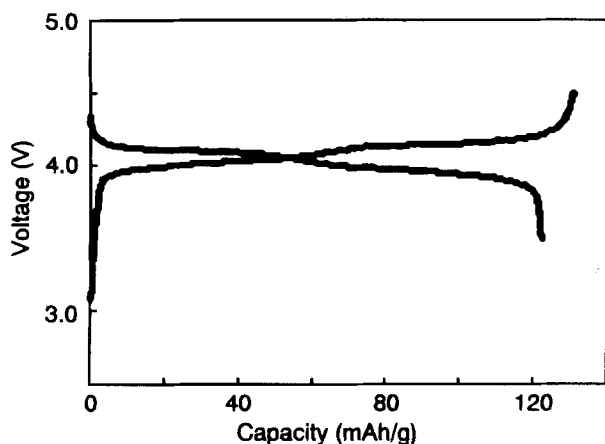


Fig. 1. Initial charge and discharge curves of a cell with a Li<sub>1.04</sub>Mn<sub>1.98</sub>O<sub>4</sub> cathode, lithium metal anode, and 1 M LiPF<sub>6</sub> in EC:DMC (1:2) at a current density of 0.5 mA/cm<sup>2</sup> at 25°C.

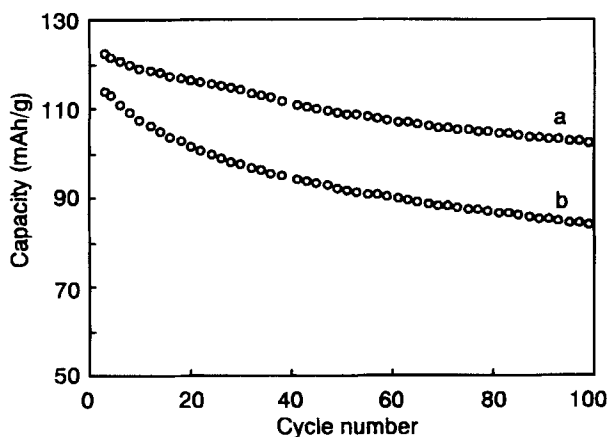
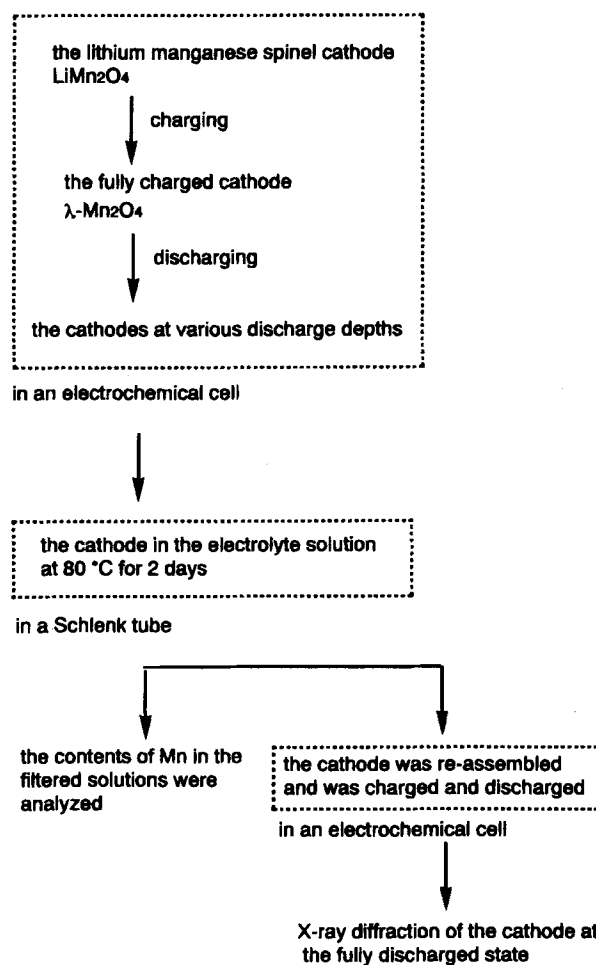


Fig. 2. Cycle performance of Li<sub>1.04</sub>Mn<sub>1.98</sub>O<sub>4</sub> cathode, lithium metal anode, and 1 M LiPF<sub>6</sub> in EC:DMC (1:2) at a current density of 0.5 mA/cm<sup>2</sup> (a) at 25 and (b) at 55°C.



Scheme 1.

room temperature. This rules out a significant effect of manganese ions in solution on the performance of the cell. Hence, the capacity loss is caused by the manganese loss from the cathode.

**Mn dissolution from the cathodes at various discharge states at 80°C.**—We examined the thermodynamic solubility of manganese ions in the spinels at various discharge depths in the electrolyte solution at 80°C as shown in Scheme 1. The cells consisted of a lithium metal anode, 1 M LiPF<sub>6</sub>-EC/DMC (1:2 by volume), and the spinel cathode. The charging of the cells was performed galvanostatically at a current density of 0.5 mA/cm<sup>2</sup> up to 4.5 V, and after a 2 h pause, the discharge was performed to each depth (0, 25, 50, 75, 100%). The cells were then disassembled.

Each cathode was exposed to 10 mL of the electrolyte solution (1 M LiPF<sub>6</sub>-EC/DMC (1:2 in volume) at 80°C for 2 days in a Schlenk tube, and then the solution was filtered in a glove box. The amounts of Mn in the solution were analyzed using the atomic absorption method. A cell with Li/electrolyte/spinel-cathode was reassembled and charged to 4.5 V. It was then discharged to 3.5 V to measure the discharge capacity of each cathode, as shown in Fig. 3. Subsequently, X-ray diffraction patterns of the cathode were recorded in Ar atmosphere.

Table I shows the weights of the cathodes, the quantities of dissolved Mn in the 10 mL electrolyte solutions, and the discharge capacities of the spinel electrodes after Mn dissolution. The quantities of the dissolved Mn in the solution ranged from 0.13 to 0.34 mg, independently based on the discharge depth of the cathodes. The maximum Mn weight loss from the cathode due to dissolution is less than 1.2%. However, in the solution without LiPF<sub>6</sub>, no trace of the dissolved Mn was detected.

Now let us focus on the discharge capacities of the electrodes. The lowest specific capacity is 50 mAh/g of the

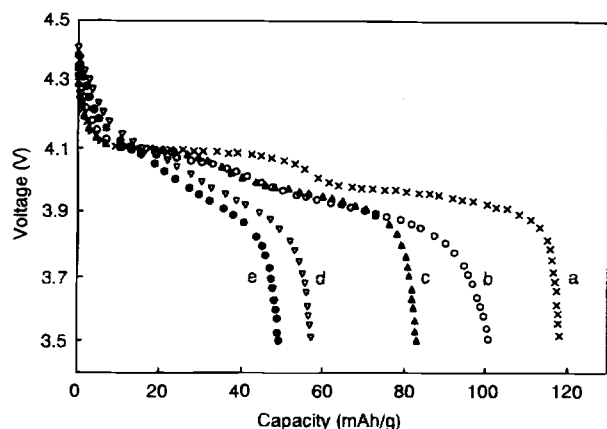


Fig. 3. Discharge curves of  $\text{Li}_{1.04}\text{Mn}_{1.98}\text{O}_4$  cathode after Mn dissolution, lithium metal anode, and 1 M  $\text{LiPF}_6$  in EC:DMC (1:2) at a current density of  $0.5 \text{ mA/cm}^2$ : a, b, c, d, and e cathodes exposed to the electrolyte at 0, 25, 50, 75, and 100% discharged states, respectively.

fully discharged cathode where the capacity loss is 59%. On the other hand, the fully charged cathode exhibits only 3% capacity fading. The discharge capacities decrease with deeper discharge states of the electrodes. It must be emphasized that storage of cells with the discharged manganese spinel at elevated temperatures causes severe capacity fading. These findings indicate that the capacity loss at elevated temperature should correlate with the existence of  $\text{Mn}^{3+}$  in the spinel.

After a dissolution test without  $\text{LiPF}_6$ , no capacity fading of the cathode was found. Therefore,  $\text{LiPF}_6$  itself and/or its decomposition products dissolve manganese from the cathode into the solution. Jang et al.<sup>16,17</sup> and Pistoia et al.<sup>11</sup> also found a lithium-salt effect on the spinel dissolution.

**X-ray diffraction studies of the cathodes after Mn dissolution.**—In order to investigate structures of the cathodes after the Mn dissolution, X-ray diffraction studies were carried out. Figure 4 shows the diffraction patterns of four cathodes at the different discharge depths in the  $2\theta$  range of  $30\text{--}80^\circ$ . When a deeper discharged cathode was soaked in the electrolyte, all diffraction peaks broadened and shifted to higher angles. New and unidentified diffraction patterns were found for the 75 and 100% discharged cathodes. Ratios of full widths at half-maximum in the 0, 50, 75, and 100% discharged cathodes are 1:1.4:1.5:1.8 for the [311] diffraction, 1:1.5:1.7:2.9 for the [400] diffraction, and 1:1.3:1.6:2.6 for the [440] diffraction, respectively, in qualitative accordance with increasing capacity loss.

**Capacity fading and disorder in the crystal structure of the cathodes.**—Now we consider the capacity fading during storage at elevated temperatures. We estimate the quantity of the discharge capacity loss due to the manganese dissolution. Table II shows the estimated values of the capacity loss according to some models. By these models, the 59% capacity loss is calculated to be caused by 10% or more Mn dissolution in the solution, and 1% Mn dissolution causes only 10% capacity loss. The estimated

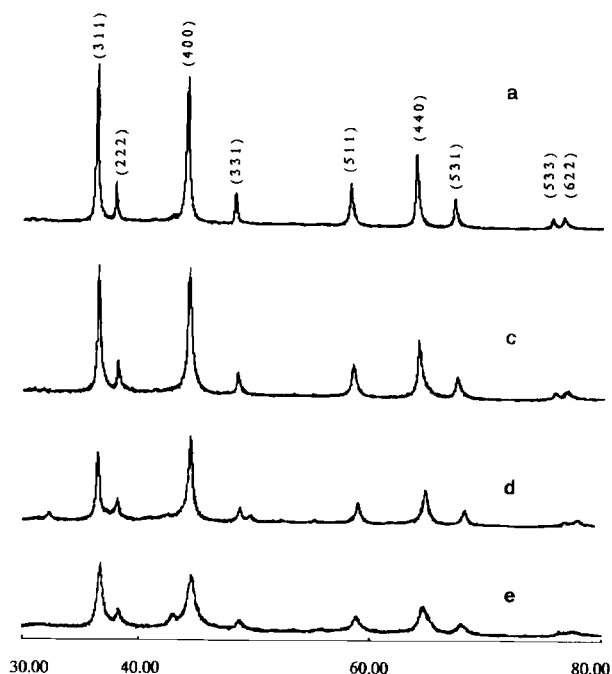


Fig. 4. X-ray diffraction patterns of the a, c, d, and e cathodes that were charged and fully discharged after Mn dissolution at 0, 50, 75, and 100% discharged states, respectively.

values are different from the experimental ones. It is obvious that the weight loss of the cathode due to the dissolved Mn does not directly cause the capacity loss, even if experimental error is considered, and it is also clear that there is no correlation between the amounts of capacity loss, and the dissolved Mn. Therefore, a reason for as little as 1% Mn dissolution causing a 60% capacity loss found in the experiment is necessary.

Let us recall the relation between the XRD peak widths and the capacity loss as described previously. The more the capacity loss increases, the more the peak widths broaden.<sup>19a</sup> Consider two candidate explanations as causes of the broader peak widths: one is structural disorder and another is a decrease in particle size in the spinel powder. The decrease in the particle size in the cathode suggests that the particles of the spinel powder split so that the resulting small particles become electrically isolated from the electrode. Addition of conductive binders to the cathode is expected to provide electrical conduction between them and the cathode, leading to recovery of the discharge capacity. In order to determine which of the two is the primary cause of the peak broadening, a conductive binder was added to the cathode after measurements of its discharge capacity, the pellet was reprepared as a cathode, and the discharge capacity was then measured. An increase in the capacity was not found. The broader peak widths is thus related to structural disorder in the spinels.

<sup>a</sup> The relation between peak broadening and capacity loss was also found in cycling at room temperature (see Ref. 19).

Table I. Weights of the cathodes, quantities of the dissolved Mn, and specific discharge capacities of the electrode after Mn dissolution.

Discharged state of the cathode	Weight of cathode (mg)	Concentration of dissolved Mn (ppm)	Quantity of dissolved Mn (10 mL)	Weight loss %	Specific discharge capacity after Mn dissolution (mAh/g)
0%	47.4	14.0	0.13	0.45	122 (0%)
25%	48.8	29.3	0.28	0.94	105 (86%)
50%	49.1	30.7	0.29	0.97	83 (82%)
75%	49.7	35.2	0.34	1.12	58 (48%)
100%	49.6	22.8	0.22	0.73	50 (41%)
100% <sup>a</sup>	49.6	Less than 1.3	Less than 0.01	Less than 0.03	122 (0%)

<sup>a</sup> The electrode was exposed to 10 mL of non- $\text{LiPF}_6$  solution [EC/DMC (1:2 in volume)] at  $80^\circ\text{C}$  for 2 days.

**Table II. Simulation of capacity loss for  $\text{Li}_{1.04}\text{Mn}_{1.98}\text{O}_4$  by manganese dissolution.**

Expected Mn loss (wt %)	Chemical formula	Theoretical capacity loss (mAh/g)	Capacity loss (mAh/g)
1% via MnO	$\text{Li}_{1.04}\text{Mn}_{1.96}\text{O}_{3.98}$	139	3 (2%)
	$\text{Li}_{1.04}\text{Mn}_{1.96}\text{O}_{3.97}$	139	3 (2%)
2% via MnO	$\text{Li}_{1.04}\text{Mn}_{1.94}\text{O}_{3.96}$	130	12 (8%)
	$\text{Li}_{1.04}\text{Mn}_{1.94}\text{O}_{3.95}$	133	9 (6%)
5% via MnO	$\text{Li}_{1.04}\text{Mn}_{1.88}\text{O}_{3.90}$	112	30 (21%)
	$\text{Li}_{1.04}\text{Mn}_{1.88}\text{O}_{3.87}$	121	21 (15%)
10% via MnO	$\text{Li}_{1.04}\text{Mn}_{1.78}\text{O}_{3.80}$	83	59 (42%)
	$\text{Li}_{1.04}\text{Mn}_{1.78}\text{O}_{3.74}$	101	41 (29%)

Disorder in the crystal structures is triggered as a result of manganese dissolution. The Li insertion-extraction paths become blocked so that a substantial capacity loss is observed even with small amounts of Mn dissolution. In other words, a direct cause of the capacity loss is the collapse of the lithium insertion-extraction paths. These barriers to the  $\text{Li}^+$  conduction were also supported by the increase in the cell resistance by ac impedance spectroscopy and the discharge capacities at low current densities. (The discharge capacity for the fully discharged cathode is 65 mAh/g at a current density of 0.05 mA/cm<sup>2</sup>.) Jang et al.<sup>10</sup> also observed polarization loss due to cell resistance increment after cycling at elevated temperature.

*Discharge depths of the cathodes and capacity loss.*—We now consider the capacity loss of the deeper discharged cathodes at elevated temperatures. Elevated temperatures promote decomposition of  $\text{LiPF}_6$ , whose products can dissolve manganese into the solution from the cathode. Also, elevated temperatures cause intense vibration of the lattices in the spinel. Manganese(III) ions with the Jahn-Teller distortion produce strains in the lattice, and larger lattices also cause looseness in the crystal. A spinel containing  $\text{Mn}^{3+}$  undergoes structural destabilization. The defects caused by the dissolved Mn trigger the destruction of the  $\text{Mn}^{3+}$ -rich lattice of the spinel. Hence, the deeper discharged cathode after Mn dissolution exhibits more disorder in its crystals, leading to more capacity fading. We should mention the fully charged cathode with little capacity loss in spite of the weight loss (0.45%) due to Mn dissolution. Crystal destruction due to the dissolution barely contributes to capacity fading due to the  $\text{Mn}^{4+}$  skeleton without the Jahn-Teller effect in  $\lambda\text{-Mn}_2\text{O}_4$ .

### Conclusions

The quantity of dissolved manganese in the 1 M  $\text{LiPF}_6$  EC/DMC (1:2 by volume) electrolyte solution was less than 1.2% of the total manganese in the spinel at 80°C for 2 days. Only a 3% capacity fading was found for the cathode in its charged state, but a 59% capacity loss was observed in its discharged cathode. A correlation between the quantities of the capacity loss and the peak widths of X-ray dif-

fraction in the spinel after the Mn dissolution was found, but no correlation between the quantity of the Mn dissolution and the quantity of the capacity loss was found. We propose a mechanism for the capacity fading due to the Mn dissolution from the spinel stored at elevated temperatures as follows: lattice defects in the spinel due to the Mn dissolution cause disorder in the crystal structure, and as a result, the Li insertion-extraction paths are blocked, leading to capacity fading.

### Acknowledgments

The authors thank Professor O. Yamamoto and Dr. S. Imanishi of Mie University for assembling the cells.

Manuscript submitted January 26, 1998; revised manuscript received June 26, 1998.

Nagoya University assisted in meeting the publication costs of this article.

### REFERENCES

- J. M. Tarascon, W. R. McKinnon, F. Coowar, T. N. Bowmer, G. Amatucci, and D. Guyomard, *J. Electrochem. Soc.*, **141**, 1421 (1994).
- V. Manev, A. Momchilov, A. Nasslevska, and A. Kozawa, *J. Power Sources*, **41**, 305 (1993).
- Y. Xia and M. Yoshio, *J. Power Sources*, **56**, 61 (1995).
- J. M. Tarascon, E. Wang, F. K. Shokoohi, W. R. McKinnon, and S. Colson, *J. Electrochem. Soc.*, **138**, 2859 (1991).
- G. Pistoia, G. Wang, and C. Wang, *Solid State Ionics*, **58**, 285 (1992).
- G. Pistoia and G. Wang, *Solid State Ionics*, **66**, 135 (1993).
- R. Bittihn, R. Herr, and D. Hoge, *J. Power Sources*, **43-44**, 223 (1993).
- G. Pistoia, A. Antonini, R. Rosati, and D. Zane, *Electrochim. Acta*, **41**, 2683 (1996).
- Y. Xia and M. Yoshio, *J. Electrochem. Soc.*, **143**, 825 (1996).
- D. H. Jang, Y. J. Shin, and S. M. Oh, *J. Electrochem. Soc.*, **143**, 2204 (1996).
- G. Pistoia, A. Antonini, R. Rosati, and C. Bellitto, in *Batteries for Portable Applications and Electric Vehicles*, A. R. Landgrebe and C. F. Holmes, Editors, PV 97-18, p. 406, The Electrochemical Society Proceedings Series, Pennington, NJ (1997).
- Y. Xia, Y. Zhou, and M. Yoshio, *J. Electrochem. Soc.*, **144**, 2593 (1997).
- G. G. Amatucci, A. Blyr, C. Schmutz, and J. M. Tarascon, *Prog. Batt. Batt. Mater.*, **16**, 1 (1997).
- Private communication.
- K. Takahashi, T. Sotomura, T. Endoh, and K. Otani, *The Battery Symposium in Japan*, 1A21, 87 (1996).
- A. M. Bond and D. R. Canterford, *Anal. Chem.*, **43**, 134 (1971).
- D. H. Jang and S. M. Oh, *J. Electrochem. Soc.*, **144**, 3342 (1997).
- A. D. Robertson, S. H. Lu, and W. F. Howard, Jr., *J. Electrochem. Soc.*, **144**, 3505 (1997).
- T. Inoue, Y. Iwaigawa, and M. Sano, *Prog. Batt. Batt. Mater.*, To be published (1998).